Chapter 21
Paint Delamination as a Result of Zinc Soap Formation in an Early Mondrian Painting

Annelies Van Loon, Ruth Hoppe, Katrien Keune, Joen J. Hermans, Hannie Diependaal, Madeleine Bisschoff, Mathieu Thoury, and Geert van der Snickt

Abstract The Evolution triptych by Piet Mondrian (1911, oil on canvas, Gemeentemuseum Den Haag) presents a case study of a painting that is seriously affected by zinc soap formation, which has resulted in paint delamination and paint loss, particularly in the cadmium yellow paint areas. The paint is extremely fragile, which makes the paintings vulnerable with regard to handling and treatment. This paper

A. Van Loon (✉)
Conservation Department, Rijksmuseum, Amsterdam, The Netherlands
e-mail: a.vanloon@rijksmuseum.nl

R. Hoppe (✉)
Gemeentemuseum Den Haag, The Hague, The Netherlands
e-mail: rhoppe@gemeentemuseum.nl

K. Keune
Conservation Department, Rijksmuseum, Van't Hoff Institute for Molecular Sciences, University of Amsterdam, Amsterdam, The Netherlands

J. J. Hermans
Van't Hoff Institute for Molecular Sciences, University of Amsterdam, Amsterdam, The Netherlands

H. Diependaal · M. Bisschoff
Independent paintings conservator, Amsterdam, The Netherlands

M. Thoury
IPANEMA, CNRS, ministère de la Culture et de la Communication, Université de Versailles Saint-Quentin-en-Yvelines, Muséum National d'Histoire Naturelle, USR 3461, Université Paris-Saclay, Gif-sur-Yvette, France

G. van der Snickt
Department of Chemistry – AXES group, University of Antwerp, Antwerp, Belgium

Conservation Studies, University of Antwerp, Antwerp, Belgium

F. Casadio et al. (eds.), *Metal Soaps in Art*, Cultural Heritage Science,
https://doi.org/10.1007/978-3-319-90617-1_21

focuses on the analytical research of the painting using various state-of-the-art and novel macro- and micro-imaging techniques. Macro X-ray fluorescence scanning (MA-XRF) revealed the presence of cadmium (Cd) and zinc (Zn) in the affected yellow paints. Paint cross sections of both affected and intact paint areas were investigated using light microscopy, scanning electron microscopy coupled with energy dispersive X-ray analysis (SEM-EDX), attenuated total reflection Fourier transform infrared (ATR-FTIR) micro-imaging, and synchrotron photoluminescence (PL) micro-imaging. With the help of these techniques, the cadmium yellow pigment could be identified as a mixture of cadmium sulfide and cadmium oxalate. The presence of zinc white was established in areas where the yellow paint film is degraded, while the intact areas of yellow paint do not contain any zinc white. In samples of the degraded paints, it was demonstrated that high concentrations of zinc soaps have formed, accumulating at interfaces. This has caused local chemical and physical changes of the paint resulting in delamination between paint layers.

Keywords Zinc soaps · Metal soaps · Paint delamination · Cadmium yellow · Mondrian

21.1 Introduction

The *Evolution* triptych by Piet Mondrian (1911, oil on canvas, 178 × 85; 183 × 87.5; 178 × 85 cm), which belongs to the artist's early period of figurative painting, is one of the most prominent works in the collection of the Gemeentemuseum Den Haag (Fig. 21.1). The triptych consists of three separate paintings that are overall surprisingly well preserved, given the fact that the paintings have survived in their original frames and are still unvarnished and not relined. The yellow paint areas in the center and left panels, however, suffer from a peculiar form of degradation, which is only visible with higher magnification (Fig. 21.2). Local wrinkling can be observed and also delamination between the top layer and the underlying paint. This occurs in the form of blistering or "tunneling," which appears to correspond with the brushstrokes of an underlying paint application. Associated paint loss can also be seen with the microscope, indicating that the yellow paint is very vulnerable and has already suffered in the past from inadequate handling and treatment. During tests for consolidation treatment, it became clear that the lifting paint breaks upon the slightest touch.

Degradation phenomena in cadmium yellow paints are a familiar problem in works by Mondrian and his contemporaries (Kolkena 2014; Van der Snickt et al. 2009, 2012; Mass et al. 2013). In the collection of the Gemeentemuseum, these problems have been identified in some later paintings dating from 1921, *Composition with Large Red Plane, Yellow, Black, Grey and Blue*, and *Composition with Red, Blue, Black, Yellow and Grey,* and only in one early painting, *Seascape*, painted in 1909. In these paintings, however, the degradation phenomena appear differently: the paint is crumbling or disintegrating, or showing discoloration.

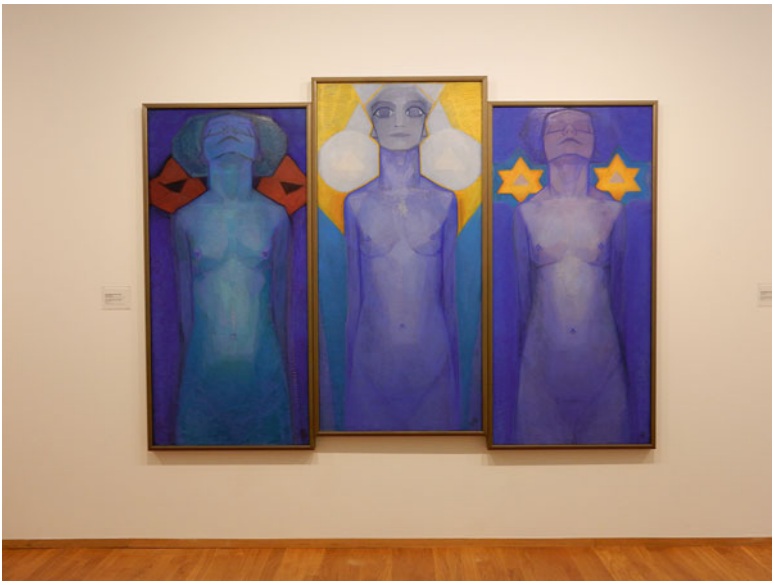

Fig. 21.1 Piet Mondrian, *Evolution*, 1911, oil on canvas, triptych: 178 × 85; 183 × 87.5; 178 × 85 cm, Gemeentemuseum Den Haag, the Netherlands. The paintings are currently presented in the galleries in three custom-made display frames

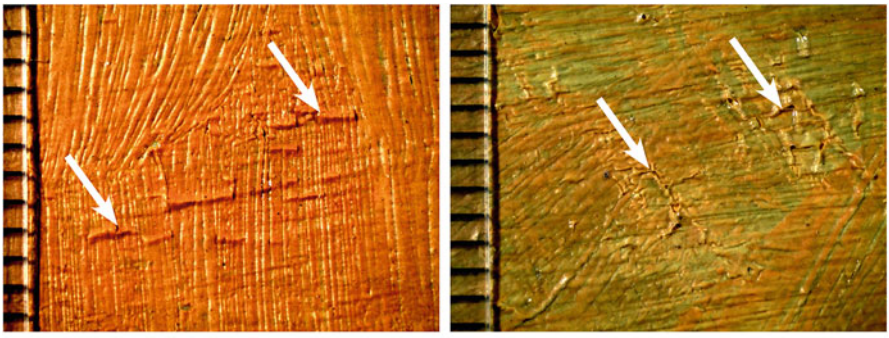

Fig. 21.2 Macrophotographs of degradation phenomena in cadmium yellow paint (**a**) tunneling and lifting across brushstroke relief; (**b**) wrinkling with associated paint loss

As part of the technical examination of the triptych, an area of 60 × 80 cm at the top right part of the center panel, including the yellow paint areas, was mapped with macroscopic X-ray fluorescence scanning (MA-XRF). This is a recent diagnostic imaging tool that reveals the elemental distributions on and below the paint surface in a non-invasive manner, thus providing information about the paint composition (Alfeld et al. 2011). Additional micro-sampling was necessary, in order to be able to fully interpret the MA-XRF data and to assess the condition of the paint. Subsequently, sample locations were carefully selected, with the aid of the XRF scans. Both affected and intact paint areas were sampled for comparison. Samples

were prepared as cross sections and investigated with light microscopy, scanning electron microscopy coupled with energy dispersive X-ray analysis (SEM-EDX), attenuated total reflection Fourier transform infrared (ATR-FTIR) micro-imaging, and synchrotron photoluminescence (PL) micro-imaging. For the ATR-FTIR measurements, a new sample accessory was used in the experimental setup, containing a germanium ATR hemisphere with a flat top part (1 mm ∅). The hemisphere has to be brought in contact with the sample surface, but the advantage is that it leaves no circular depressions in the sample, as conventional ATR crystals do. Synchrotron PL was used here as a novel approach to visualize alteration products in the paint layers at high, submicron spatial resolution, based on their specific luminescence properties (see also Thoury et al. 2019). Since the most affected areas in the painting are in the yellows, the first thought was that the degradation would be related to the use of a cadmium yellow pigment. The combined chemical analyses, however, revealed that the major cause of the delamination is zinc soap formation, as discussed in this paper.

21.2 Experimental

21.2.1 MA-XRF

Macroscopic X-ray fluorescence maps were collected using a Bruker M6 Jetstream Instrument (Alfeld et al. 2013). This instrument consists of a measuring head on an XY-motorized stage that is slowly moved over the surface of the painting (no actual contact is made with the paint surface), scanning the painting pixel by pixel and line by line. The measuring head consists of a Rh-target microfocus X-ray tube (30 W, maximum voltage 50 kV, maximum current 0.6 mA) and a 30 mm^2 XFlash silicon drift detector (energy resolution <145 eV at Mn-Kα). The beam size is defined by means of a polycapillary optic and is variable, determined by the distance between the paint surface and the measuring head (varying between 150 μm at 6 mm working distance and 860 μm at 15 mm working distance). For the Mondrian painting, element distribution maps were collected over an area measuring 767 by 578 mm^2 (1096 by 826 pixels) in a single 24 h session. X-ray tube settings were 50 kV and 600 μA; a step size of 700 μm, a dwell time of 70 ms/step, and a beam size estimated to be 350 μm in diameter were used. All data were collected with the Bruker M6 Jetstream software package. The acquired spectra were then exported and processed using PyMca and the in-house developed Datamuncher software (Alfeld and Janssens 2015).

21.2.2 Microanalyses

21.2.2.1 Samples

Five micro-samples were taken in total from the center panel (Fig. 21.3a) (from the area scanned with XRF) for comparison. They were all taken along the edges of

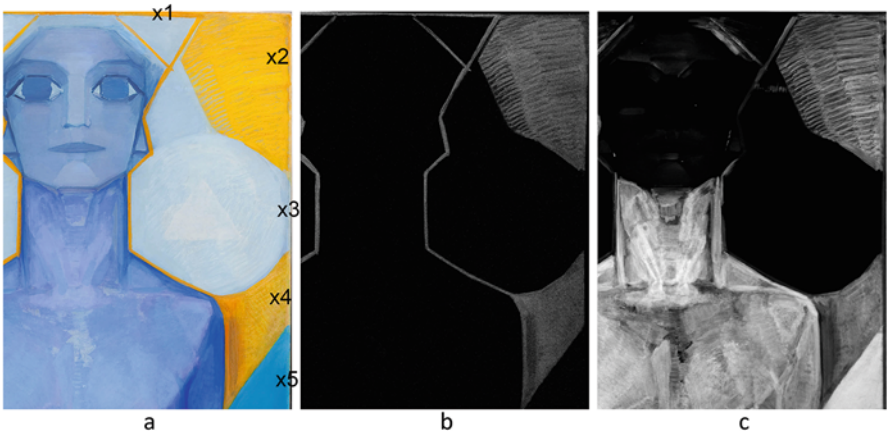

Fig. 21.3 Macro-XRF scanning of the top right part of the center panel: (**a**) area scanned with MA-XRF. With the aid of the XRF scans, sample sites (X1–5) were selected from intact and degraded areas for further analysis; (**b**) cadmium (Cd-L) map (higher brightness indicates higher signal); (**c**) zinc (Zn-K) map

the painting, with the aid of the stereo-microscope, from areas of both intact and degraded paint (Table 21.1).

21.2.2.2 Sample Preparation

The paint micro-samples were embedded in Technovit 2000 LC mounting resin, a one-component methacrylate that polymerizes under visible blue light (Heraeus Kulzer GmbH, Germany). They were wet-polished on a polishing machine to expose the complete paint layer buildup, with the assistance of a sample holder. The final polishing steps were done with Micromesh sheets up to grade 12,000 (Micro-Surface Finishing Products Inc., Wilton, Iowa, USA), using the dry polishing method (Van Loon et al. 2005).

21.2.2.3 Light Microscopy

Light microscopic (LM) studies of the paint cross sections were performed on a Leica DMRX microscope at the FOM Institute AMOLF in Amsterdam. The cross sections were examined at magnifications up to 1000×, in normal incident light, in bright-field (BF) (with and without oil immersion) and in dark-field illuminations, and with ultraviolet (UV-A) using Leica filters A (excitation 340–380 nm, emission >425 nm) and D (exc. 355–425 nm, em. >470 nm).

Table 21.1 Summary of the cross-sectional analyses

Sample no.	Sample location	XRF	Paint composition and buildup	Microanalyses
X1	Yellow border along the top edge. Paint is intact	Cd, Pb	2. Yellow paint: cadmium yellow (CdS and Cd-oxalate), very little chalk 1. White ground: lead white	LM, SEM-EDX
X2	Yellow paint area at upper right, from a pastose brushstroke. Showing wrinkling	Cd, Zn, Pb	4. Yellow paint: cadmium yellow, zinc white (*zinc soap formation*) 3. Light-blue paint: lead white, single particle of synth. ultramarine 2. Blue paint: lead white, synth. ultramarine, barium sulfate 1. White ground: lead white	LM, SEM-EDX, ATR-FTIR, PL
X3	Light-blue paint area. Paint is intact	Pb	5. Light-blue paint: lead white, few blue particles 4. Blue paint: lead white, fine blue pigment (same as in layer 2) 3. Light-blue paint: lead white, single blue particle 2. Blue paint: lead white, fine blue pigment 1. White ground: lead white	LM
X4	Pale yellow paint area, next to paint loss. Showing paint delamination and wrinkling	Cd, Zn, Pb	8. Pale yellow paint: zinc white, cadmium yellow, single particle of blue (*zinc soap formation*) 7. Yellow paint: cadmium yellow (CdS and Cd-oxalate), very little chalk 6. Blue paint: lead white, blue pigment, few pale-reddish particles 5. Light-blue paint: lead white, some blue pigment 4. Blue paint: lead white, lots of blue pigment 3. Light-blue paint: lead white, single blue particle 2. Light-blue paint: lead white, some blue pigment 1. White ground: lead white	LM, SEM-EDX, ATR-FTIR, PL
X5	Turquoise blue paint area. Slightly deformed paint	Fe, Cr, Zn	7. Blue paint: zinc white, fine blue pigment (*zinc soap formation*) 6. Green-blue paint: zinc white, cadmium yellow, few blue-green particles (*zinc soap formation*) 5. Yellow paint: cadmium yellow (CdS and Cd-oxalate), very little chalk 4. Blue paint: lead white, fine blue 3. Light-blue paint: lead white, some blue pigment 2. Blue paint: lead white, fine blue pigment 1. White ground: lead white	LM, SEM-EDX

21.2.2.4 SEM-EDX

SEM-EDX analysis of the embedded samples was performed at the FOM Institute AMOLF in Amsterdam, using a FEI Verios 460 high-pressure electron microscope equipped with an Oxford EDX system. Backscattered electron images were acquired at 20 kV acceleration voltage and 0.20 nA beam current. EDX spectral maps were recorded at the same kV and beam current, with 1024 × 640 pixels resolution and 100 μs dwell time. The samples were gold coated (3 nm) on an SC7640 sputter coater (Quorum Technologies, Newhaven, East Sussex, UK) prior to analysis to improve surface conductivity.

21.2.2.5 ATR-FTIR Micro-imaging

ATR-FTIR measurements were undertaken at the IPANEMA Laboratory, on a Bruker Hyperion 3000 FTIR microscope using a focal plane array (FPA) detector, coupled to a VERTEX 70 FTIR spectrometer. An ATR hemisphere sample accessory was used, equipped with a base germanium hemisphere crystal with a 1 mm diameter flat top that is brought in contact with the sample. The spectra were collected with 4 cm^{-1} spectral resolution in the range 4000–900 cm^{-1} averaging 128 scans. Data were processed using the OPUS 7.2 software.

21.2.2.6 Synchrotron-Photoluminescence Micro-imaging

PL experiments were accomplished on the DISCO beamline at Synchrotron SOLEIL using the full-field micro-imaging setup (TELEMOS) (Giuliani et al. 2009; Bertrand et al. 2013). The excitation wavelength was set at 280 nm. The use of a 100 × 1.25 NA ultrafluar objective allowed collecting images up to 250 nm spatial resolution. Images were acquired in nine spectral bands between 327 and 870 nm using high transmittance band-pass interference filters. The intensity of each channel of the full-field RGB image was stretched between the 2nd and 98th percentile using the ENVI 5.0 software (EXELIS) to facilitate visual comparison.

21.3 Results

21.3.1 Macro-XRF Scanning

In the context of this study, the cadmium (Cd-L) and zinc (Zn-K) distribution maps are the most informative; see Fig. 21.3b, c, respectively. The Cd map indicates the use of a cadmium-containing pigment in the yellow paint areas, in the two large areas at the right part of the XRF scan, and in the yellow lines following

the contours of the face and neck and along the top edge of the painting. Zinc is also abundantly present in the degraded areas of yellow paint, particularly in the two large areas. Zinc is absent in the yellow border along the top edge, where the paint film is intact. Interestingly, the XRF scan reveals significantly high amounts of zinc in the turquoise blue paint area at the lower right corner of the scan, where the paint film shows a certain degree of deformation, whereas in the intact light blue paint area at the center right part, no zinc, only lead, was detected. This points to a causal connection between the presence of zinc and the degradation of the paint. The MA-XRF maps alone did not permit the exact zinc source to be pinpointed. In particular, it remained unclear whether the detected zinc originated from a cadmium zinc sulfide pigment or from the admixture of a separate zinc compound (pigment or drier) to the paint. Paint cross-sectional analysis was expected to shed further light on this and on the paint buildup, as well as identify possible degradation products. In this framework, the MA-XRF maps proved to be particularly helpful for selecting good sample spots and thus for keeping the number of samples to a minimum.

21.3.2 Cross-Sectional Analyses

The findings arising from all the studied micro-samples are summarized in Table 21.1. Two representative samples will be discussed here in detail: sample X1 taken in an intact yellow paint area and sample X4 originating from a degraded yellow paint area.

21.3.2.1 Intact Yellow Paint (X1)

Sample X1 is taken from the yellow border at the top edge of the painting, where the paint film is thin and appears intact (Fig. 21.4a). In this area only cadmium and lead were detected with MA-XRF; zinc is absent. The light microscopic image of the cross section shows a simple layer buildup (Fig. 21.4b): a lead white ground followed by a thin, evenly applied yellow paint layer (thickness *c.*20 μm). The yellow layer contains cadmium yellow pigment only, without any addition of zinc white or other pigments. The absence of zinc white is supported by the UV-A image, in which the typical fluorescent "sparks" of zinc white cannot be observed (Fig. 21.4c). SEM-EDX analysis revealed the presence of cadmium and sulfur in the yellow paint; no zinc was detected (Fig. 21.4d-f). Therefore it can be presumed that the cadmium yellow pigment is cadmium sulfide and not cadmium zinc sulfide. The same paint is present in sample X4 as an underlayer (layer 7) where analysis shows the cadmium sulfide pigment is mixed with larger chunks of cadmium oxalate (see section "Degraded Yellow Paint (X4)"). Although cadmium oxalate has been identified as a degradation product in other studies (Van der Snickt et al. 2009, 2012; Mass et al. 2013), in this case it is not a degradation product but an original paint component.

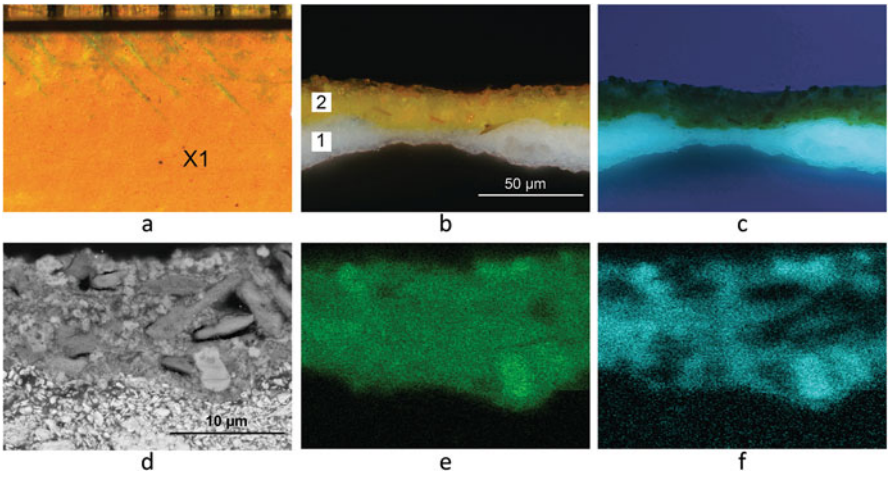

Fig. 21.4 Cross-section analyses of intact yellow paint (X1): (**a**) sample location (X1): yellow border at top edge, where the paint is intact; (**b**) light microscopic image of paint cross section in normal light (BF, oil immersion), photographed at 400×; (**c**) cross section in ultraviolet light (UV-A); (**d**) SEM backscatter image, zoomed in on the yellow paint; (**e**) EDX cadmium map of (d); (**f**) EDX sulfur map of (d)

21.3.2.2 Degraded Yellow Paint (X4)

Sample X4 represents a degraded yellow paint area. It was taken from a spot just next to an area where the top part of the paint layers had already delaminated, in order to make sure that the sample would contain all layers (Fig. 21.5a[1]).

The cross section shows a thick, multilayered package. It contains several underlayers of lead white and blue paint (these are not visible in the images). Figure 21.5b shows the top layers only, where the delamination takes place.[2] A thin yellow paint layer (7) (thickness *c.*15–20 µm) comprising purely cadmium yellow pigment is followed by a thick, pale yellow paint layer (8) (thickness up to *c.*60 µm), which contains a lot of zinc white and little cadmium yellow. Translucent areas are noticeable in layer 8, especially at the surface and at the interface with paint layer 7 below. In ultraviolet light (UV-A), the same layer shows numerous tiny, strongly fluorescent particles characteristic of zinc white (Fig. 21.5c). The fluorescent "sparks" are absent in the translucent areas, which suggests that the

[1]LM and SEM-EDX were done prior to ATR-FTIR and PL micro-imaging. When re-polishing the sample to remove the 3 nm-thick gold coating applied for the SEM-EDX analysis, the surface was slightly modified. This explains why the images obtained with the different analytical techniques cannot be 100% overlayed.

[2]During sampling, the thick paint broke into two halves, which were embedded separately. The sample containing the lower part of the layer structure was also analyzed, but the images are not shown here since those layers do not show any sign of degradation and appear stable.

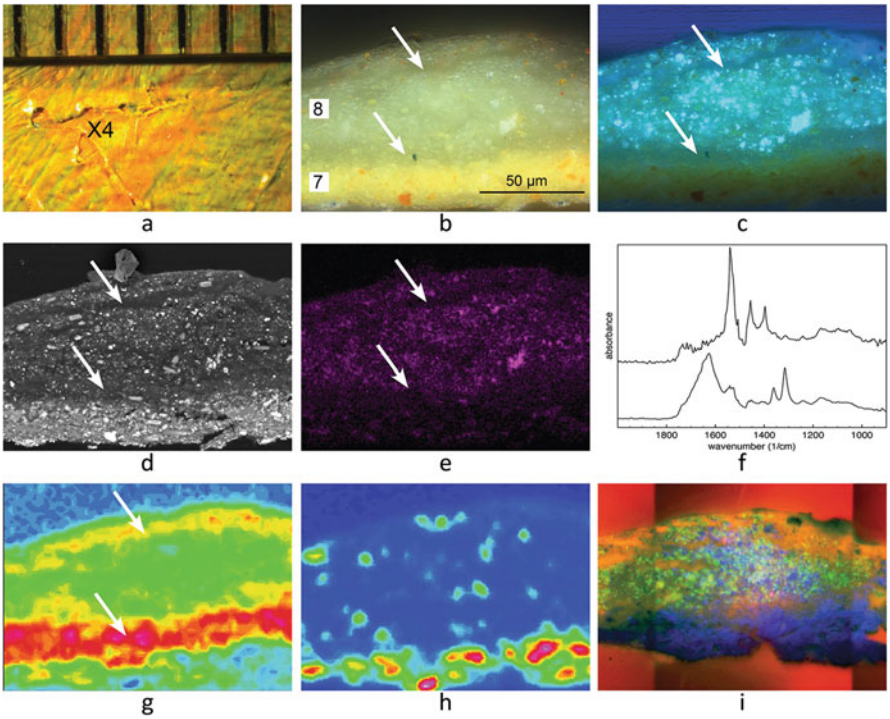

Fig. 21.5 Cross-section analyses of degraded yellow paint (X4): (**a**) sample location (X4): yellow paint area showing delamination (wrinkling); (**b**) light microscopic image of paint cross section in normal light (BF, oil immersion, photographed at 400×). The sample shows top layers only, where the delamination takes place. The white arrows point to the translucent areas in paint layer 8; (**c**) cross section in ultraviolet light (UV-A); (**d**) SEM backscatter image; (**e**) EDX zinc map; (**f**) ATR-FTIR spectra. Upper trace: spectrum from pale yellow top layer (8) showing characteristic zinc soap peaks. Lower trace: spectrum from lower yellow layer (7) showing characteristic cadmium oxalate peaks; (**g**) ATR-FTIR image of the *c.*1540 cm^{-1} band in false color, showing the distribution of zinc soaps in the pale yellow top paint layer (8) (yellow/red zones); (**h**) ATR-FTIR image of the *c.*1315 cm^{-1} band in false color, showing the distribution of cadmium oxalate particles in the yellow underlayer (7) (red zones); (**i**) photoluminescence RGB composite at 280 nm excitation (UV-C) with different emission filters. Blue channel, emission 800–870 nm, indicative of cadmium yellow pigment. Green channel, em. 370–410 nm, indicative of zinc white. Red channel, em. 327–353 nm, indicative of zinc soaps

original zinc white has dissolved or been altered in these areas. SEM backscattered electron imaging reveals that the top layer (8) is physically disrupted (Fig. 21.5d). The translucent areas are low scattering (dark) and therefore interpreted as organic-rich. What appears as small (dark) "cracks" are also filled with organic-rich material. The EDX zinc map confirms the presence of zinc in layer 8 (Fig. 21.5e). The zinc is not associated with the cadmium pigment. Thus it can be ruled out that the zinc is present in the form of cadmium zinc sulfide; it is clear that zinc white is mixed into the top paint layer (8) in high quantities. The results of light microscopic and

SEM-EDX analyses also suggest that the zinc white is in the process of reacting with the medium, converting into zinc soaps, prompting further investigation with ATR-FTIR. Zinc white is known to be very reactive toward fatty acid compounds from the oil medium resulting in the formation of zinc soaps.

ATR-FTIR micro-imaging of the cross section was carried out to characterize the translucent areas and to reveal the zinc soap distribution within the paint. The ATR-FTIR spectra demonstrate the presence of zinc soaps in the top layer (8) (Fig. 21.5f, upper trace). The spectra show an intense, sharp absorption band at *c.*1540 cm^{-1} that is characteristic of the asymmetric stretch vibration of the zinc carboxylate group $\nu_{as}(COO^-)$ in crystalline form, together with other characteristic features: the symmetric stretch vibration $\nu_s(COO^-)$ at c.1397 cm^{-1} and the C-H bend vibration δ(C-H) at *c.*1456 cm^{-1} (Hermans et al. 2014). The FTIR image of the *c.*1540 cm^{-1} band shows the distribution of zinc soaps in the paint (Fig. 21.5g). It reveals high concentrations of zinc soaps that correspond with the translucent areas in the top layer (8), especially at the paint surface and at the interface with underlying paint (layer 7). This is a very significant result, since the accumulation of zinc soaps at the interface can be directly related to the paint delamination. The conversion of the paint into zinc soaps changes its chemical and physical properties, which may cause the paint to lose adhesion with the layer below, resulting in delamination of the paint film.[3] Accumulation of zinc soaps at the lower part of a paint layer has also been found in zinc white paint reconstructions in a recent study (Osmond et al. 2012). A similar trend is apparent in other case studies of paint delamination and paint loss associated with zinc soaps in modern oil paintings, including previously published studies (Rogala et al. 2010; Helwig et al. 2014) and in other contributions to this volume (Raven et al. 2019; Osmond 2019).

ATR-FTIR micro-imaging also proved a useful tool for identifying the exact composition of the cadmium yellow pigment. Apart from cadmium sulfide, the purely yellow paint layers of X1 (layer 2) and X4 (layer 7) contain coarser particles, which are also cadmium-based but do not contain sulfur (EDX analysis). The ATR-FTIR spectra of X4 reveal absorption bands at *c.*1626 cm^{-1} (strong, broad), *c.*1361 cm^{-1} (medium, sharp) and *c.*1315 cm^{-1} (strong, sharp), which are characteristic for cadmium oxalate (Mass et al. 2013) (Fig. 21.5f. lower trace). Imaging these bands demonstrates that they correspond with the coarser particles (high cadmium/no sulfur) in the yellow underlayer (7), thus confirming the identification of cadmium oxalate (Fig. 21.5h). Since the pure cadmium yellow paint layers appear unaltered and show homogeneous mixtures of cadmium sulfide and cadmium oxalate pigment particles, it can be concluded that the latter are present as an original paint component, rather than a degradation product. At the

[3]In sample X5, which was taken from turquoise blue paint that showed some wrinkling (Table 21.1), zinc soap formation is visible at the interface between an underlying, zinc white-containing green-blue paint layer and a cadmium yellow paint layer. However, possibly due to its thickness, the turquoise blue top paint layer appears to have prevented the paint from developing more serious degradation phenomena and lifting off, at least for the time being. Due to length restrictions of this paper, sample X5 is not further discussed here.

time, cadmium oxalate was intentionally used as filler in the manufacture of paler shades of cadmium yellow paints (Fiedler and Bayard 1986).

Finally we will discuss the photoluminescence (PL) images of X4, acquired at 280 nm excitation using various emission filters ranging from 327 up to 870 nm. Three different spectral ranges are presented in the RGB composite plotted in Fig. 21.5i. Since the cadmium yellow, zinc white, and zinc soaps present in the paint layers are each shown with a different PL marker that has a specific spectral range, they can be clearly distinguished with this approach. The 800–870 nm emission image (blue channel in RGB composite) is induced by a trap state emission from cadmium sulfide (CdS), and it can be used as a characteristic signature for the cadmium yellow pigment (Thoury et al. 2011). It reveals that the cadmium yellow pigment is everywhere, including in layer 8, but not in the small "cracks" that are visible in this layer. The 370–410 nm emission image (green channel) is related to the band edge emission of zinc oxide (ZnO), and it can be used to map the presence of zinc white in layer 8 (Bertrand et al. 2013). The image shows that zinc white is present only in the top layer (8), in varying amounts. There is no indication for its presence in the lower paint layer (7). Less zinc white luminescence is visible in the top and bottom parts of layer 8 and in the "cracks," which all correspond to high-intensity areas of zinc soaps in the FTIR image. The typical fluorescent sparks of zinc white could also be recognized with conventional UV-A microscopy (see Fig. 21.5c), but the image obtained with the PL synchrotron experiment using a high numerical aperture objective centered on the band edge emission allows a more specific visualization of ZnO particles and thus reveals more details. The 327–353 nm emission image (red channel) can be indicative of zinc soaps (see also Thoury et al. 2019). The luminescence is most intense in the "cracks," where no cadmium yellow is present, showing that the "cracks" are filled with zinc soaps. In other areas, the luminescence emitted by the zinc soaps may partly be reabsorbed by the cadmium yellow pigment, resulting in lower luminescence intensity than might be expected from the ATR-FTIR imaging. This could explain why the zinc soap concentrations at the interface between layer 7 and 8 appear less bright than in the cracks. Nevertheless the emission image confirms that the zinc soaps are present throughout the whole layer. The photoluminescence data complement the FTIR imaging data. It demonstrates the specification capabilities of luminescence imaging to visualize different paint components and alteration products within a paint sample at submicron spatial resolution, which cannot be revealed with conventional UV-A microscopy.

21.4 Stages in Zinc Soap Delamination

From the chemical analyses, it can be concluded that the presence of zinc white and associated zinc soap formation must be held responsible for the paint delamination in Mondrian's *Evolution* triptych. The sample from the degraded yellow paint area X4 represents an intermediate phase in the delamination process. The paint has not

yet delaminated or fallen off, but the zinc soap formation is already in an advanced state, and its distribution in the paint layer is such that we can identify the potential weak spots in the paint structure. Why zinc soaps preferentially form or concentrate at layer interfaces is the topic of ongoing research.

21.5 Conservation Measures

In 2013, the *Evolution* triptych underwent conservation treatment. The main objective of the treatment was to stabilize the fragile paint areas in order to minimize the risk of future damage or loss of original material. For consolidation, a 15% solution of Paraloid B72 dissolved in Shellsol A was locally applied in these areas using a fine sable brush. Re-adhering lifting paint was not an option, because any attempt to apply even the slightest pressure would cause the extremely delicate paint to break. The conservation treatment included the removal of surface dirt in non-affected areas, as well as filling and retouching of minor paint loss. For reasons of protection, it was decided that the works should be presented behind glass or Perspex. Since it proved impossible to fit glazing in the narrow profile of the original frames, the paintings are now presented in the galleries in three custom-made display frames constructed from aluminum with low-reflective, shatter-proof glass and rigid backing (Fig. 21.1). Great efforts have been made to match as closely as possible the profile and coloring of the original framing. A restrictive loan policy should ensure that handling and traveling are kept to a minimum.

21.6 Conclusion

The results of the combined chemical analyses discussed in this paper have made evident that the peculiar form of degradation observed in the yellow paint areas of Mondrian's *Evolution* triptych is related to the use of zinc white in the paint and to the formation of zinc soaps and not the result of cadmium yellow degradation, as was initially thought. Zinc soaps often appear to accumulate at the lower part of a layer, at the interface with an underlying paint layer or ground, which eventually can lead to paint delamination. The case study shown here is a clear example of this phenomenon.

Acknowledgments This research is part of the Paint Alterations in Time project (PAinT), which is financially supported by the Science4Arts Programme of the Netherlands Organization for Scientific Research (NWO). The synchrotron photoluminescence experiments were carried out at the DISCO beamline, at Synchrotron SOLEIL, with the help of Matthieu Réfrégiers. Macro-XRF scanning was made possible with the support from the Baillet-Latour fund. We would also like to thank Prof. Joris Dik, Delft University of Technology, for making the Bruker M6 scanner available.

References

Alfeld M, Janssens K (2015) Strategies for processing mega-pixel X-ray fluorescence hyperspectral data: a case study on a version of Caravaggio's painting *Supper at Emmaus*. J Anal At Spectrom 30:777–789. https://doi.org/10.1039/c4ja00387j

Alfeld M, Janssens K, Dik J, de Nolf W, Van der Snickt G (2011) Optimization of mobile scanning macro-XRF systems for the in situ investigation of historical paintings. J Anal At Spectrom 26:899–909. https://doi.org/10.1039/C0JA00257G

Alfeld M, Vaz Pedroso J, Van Eikema Hommes M, Van der Snickt G, Tauber G, Blaas J, Haschke M, Erler K, Dik J, Janssens K (2013) A mobile instrument for in situ scanning macro-XRF investigation of historical paintings. J Anal At Spectrom 28:760–767. https://doi.org/10.1039/c3ja30341a

Bertrand L, Réfrégiers M, Berrie B, Échard J-P, Thoury M (2013) A multiscalar photoluminescence approach to discriminate among semiconducting historical zinc white pigments. Analyst 138:4463–4469. https://doi.org/10.1039/c3an36874b

Fiedler I, Bayard MA (1986) Cadmium yellows, oranges and reds. In: Feller RL (ed) Artists' pigments: a handbook of their history and characteristics. Cambridge University Press, National Gallery of Art, Washington, pp 65–108

Giuliani A, Jamme F, Rouam V, Wien F, Giorgetta J-L, Lagarde B, Chubar O, Bac S, Yao I, Rey S, Herbeux C, Marlats JL, Zerbib D, Polack F, Réfrégiers M (2009) DISCO: a low-energy multipurpose beamline at synchrotron SOLEIL. J Synchrotron Radiat 16:835–841

Helwig K, Poulin J, Corbeil M-C, Moffatt E, Duguay D (2014) Conservation issues in several twentieth-century Canadian oil paintings: the role of zinc carboxylate reaction products. In: Issues in contemporary oil paint. Springer, Switzerland, pp 167–184

Hermans JJ, Keune K, Van Loon A, Stols-Witlox M, Corkery R, Iedema P (2014) The synthesis of new types of lead and zinc soaps: a source of information for the study of oil paint degradation. In Bridgland J (ed) ICOM committee for conservation 17th triennial conference preprints, Melbourne, 15–19 Sept 2014, pp 1604–1612

Kolkena L (2014) A phenomenological atlas of degradation of cadmium yellow paint in paintings by Piet Mondrian (1872–1944) and some of his contemporaries, Master Thesis University of Amsterdam

Mass J, Sedlmair J, Schmidt Patterson C, Carson D, Buckley B, Hirschmugl C (2013) SR-FTIR imaging of the altered cadmium sulfide yellow paints in Henri Matisse's Le Bonheur de vivre (1905–6) – examination of visually distinct degradation regions. Analyst 138:6032–6043. https://doi.org/10.1039/c3an00892d

Osmond G (2019) Zinc soaps: an overview of zinc oxide reactivity and consequences of soap formation in oil-based paintings. In: Casadio F, Keune K, Noble P, Van Loon A, Hendriks E, Centeno S, Osmond G (eds) Metal soaps in art: conservation and research. Springer, Cham, pp 25–43

Osmond G, Boon JJ, Puskar L, Drennan J (2012) Metal stearate distributions in modern artists' oil paints: surface and cross-sectional investigation of reference paint films using conventional and synchrotron infrared microspectroscopy. Appl Spectrosc 66(10):1136–1144

Raven L, Bisschoff M, Leeuwestein M, Geldof M, Hermans JJ, Stols-Witlox M, Keune K (2019) Delamination due to zinc soap formation in an oil painting by Piet Mondrian (1872–1944). In: Casadio F, Keune K, Noble P, Van Loon A, Hendriks E, Centeno S, Osmond G (eds) Metal soaps in art: conservation and research. Springer, Cham, pp 345–357

Rogala D, Lake S, Maines C, Mecklenburg M (2010) Condition problems related to zinc oxide underlayers: examination of selected abstract expressionist paintings from the collection of the Hirshhorn Museum and Sculpture Garden, Smithsonian Institution. J Am Inst Conserv 49:96–113

Thoury M, Delaney JK, de la Rie ER, Palmer M, Morales K, Krueger J (2011) Near-infrared luminescence of cadmium pigments: in situ identification and mapping in paintings. Appl Spec 68(5):939–951

Thoury M, Van Loon A, Keune K, Réfrégiers M, Hermans JJ, Berrie BH (2019) Photoluminescence micro-imaging sheds new light on the development of metal soaps in oil paintings. In: Casadio F, Keune K, Noble P, Van Loon A, Hendriks E, Centeno S, Osmond G (eds) Metal soaps in art: conservation and research. Springer, Cham, pp 213–226

Van der Snickt G, Dik D, Cotte M, Janssens K, Jaroszewicz J, De Nolf W, Groenewegen J, van der Loeff L (2009) Characterization of a degraded cadmium yellow (CdS) pigment in an oil painting by means of synchrotron radiation based X-ray techniques. Anal Chem 81(7):2600–2610. https://doi.org/10.1021/ac802518z

Van der Snickt G, Janssens J, Dik J, De Nolf W, Vanmeert F, Jaroszewicz J, Cotte M, Falkenberg G, van der Loeff L (2012) Combined use of synchrotron radiation based micro-X-ray fluorescence, micro-X-ray diffraction, micro-X-ray absorption near-edge, and micro-Fourier transform infrared spectroscopies for revealing an alternative degradation pathway of the pigment cadmium yellow in a painting by van Gogh. Anal Chem 84(23):10221–10228. https://doi.org/10.1021/ac3015627

Van Loon A, Keune K, Boon JJ (2005) Improving the surface quality of paint cross-sections for imaging analytical studies with specular reflection FTIR and static-SIMS. In: Proceedings of Art'05 conference on non-destructive testing and microanalysis for the diagnostics and conservation of the cultural and environmental heritage, Lecce, 15–19 May 2005 (CD-ROM)